PNAS RESEARCH ARTICLE | PHYSICS

The dynamics of unsteady frictional slip pulses

Anna Pomyalov[a], Fabian Barras[b,c], Thibault Roch[d], Efim A. Brener[e,f,1], and Eran Bouchbinder[a,1]

Edited by Jay Fineberg, Hebrew University of Jerusalem, Jerusalem, Israel; received June 4, 2023; accepted July 19, 2023, by Editorial Board Member Herbert Levine

Self-healing slip pulses are major spatiotemporal failure modes of frictional systems, featuring a characteristic size $L(t)$ and a propagation velocity $c_p(t)$ (t is time). Here, we develop a theory of slip pulses in realistic rate- and state-dependent frictional systems. We show that slip pulses are intrinsically unsteady objects—in agreement with previous findings—yet their dynamical evolution is closely related to their unstable steady-state counterparts. In particular, we show that each point along the time-independent $L^{(0)}(\tau_d) - c_p^{(0)}(\tau_d)$ line, obtained from a family of steady-state pulse solutions parameterized by the driving shear stress τ_d, is unstable. Nevertheless, and remarkably, the $c_p^{(0)}[L^{(0)}]$ line is a dynamic attractor such that the unsteady dynamics of slip pulses (when they exist)—whether growing ($\dot{L}(t) > 0$) or decaying ($\dot{L}(t) < 0$)—reside on the steady-state line. The unsteady dynamics along the line are controlled by a single slow unstable mode. The slow dynamics of growing pulses, manifested by $\dot{L}(t)/c_p(t) \ll 1$, explain the existence of sustained pulses, i.e., pulses that propagate many times their characteristic size without appreciably changing their properties. Our theoretical picture of unsteady frictional slip pulses is quantitatively supported by large-scale, dynamic boundary-integral method simulations.

self-healing slip pulses | frictional rupture | spatiotemporal instabilities | earthquakes physics | geophysics

Frictional systems, such as geological faults and the tectonic plates that form them, undergo interfacial failure through various spatiotemporal rupture modes that mediate rapid sliding. The main rupture modes are known to be expanding crack-like rupture and self-healing slip pulses (1, 2). Self-healing slip pulses are solitonic structures that feature a characteristic size (compact support) $L(t)$ and a propagation velocity $c_p(t)$, where t is time (3–25). The existence of self-healing slip pulses—having no counterparts in the tensile failure of materials—crucially depends on the nonequilibrium nature of frictional interfaces, most notably on the ability of contact interfaces to recover their strength after undergoing sliding-induced weakening, i.e., to self-heal (26–32).

Frictional slip pulses pose significant physical and mathematical challenges; even obtaining steady-state pulse solutions for realistic, laboratory-derived interfacial constitutive relations and studying their dynamic stability remain major open challenges. Previous work has shown that steady-state slip pulses are unstable objects (5, 21, 22). At the same time, observations show that slip pulses can be dynamically sustained, i.e., to propagate over distances that are much larger than their characteristic size without appreciably changing their shape and propagation velocity (17, 21). This combined evidence may appear intrinsically conflicting, reflecting the lack of current understanding of the dynamics of unsteady frictional slip pulses. This problem is of prime importance in fields such as nonequilibrium and nonlinear physics, materials physics, tribology, and geophysics.

Here, we develop a theoretical picture of unsteady frictional slip pulses and reveal a surprising intrinsic relation between them and their unstable steady-state counterparts. Generic rate-and-state dependent frictional systems admit a family of steady-state slip pulse solutions parameterized by the driving shear stress τ_d, featuring a size-velocity $L^{(0)}(\tau_d) - c_p^{(0)}(\tau_d)$ relation (the superscript $^{(0)}$ refers to time-independent steady-state pulse solutions) (25). We show that each point along the $c_p^{(0)}[L^{(0)}]$ line is unstable. That is, slightly perturbed steady-state pulses either grow in time ($\dot{L}(t) > 0$) or decay ($\dot{L}(t) < 0$) such that steady-state pulses correspond to a saddle configuration. Yet, the resulting unsteady slip pulses (when they are excited, and not crack-like rupture) do not follow arbitrary dynamics in the $L(t) - c_p(t)$ plane as a function of time but are rather

Significance

A prominent failure mode of frictional systems, such as contacting tectonic plates in the earth's crust and the geological faults separating them, is self-healing slip pulses. Slip pulses, e.g., propagating along geological faults during earthquakes, feature a finite size that emerges from an interplay between leading-edge contact breakage and trailing-edge contact healing. Here, we develop a comprehensive understanding of frictional slip pulses. We show that slip pulses are intrinsically unstable objects, yet their unsteady dynamics are slow and inherently related to their steady-state counterparts. This deep relation allows us to understand the dynamical behaviors of pulses, whether growing or decaying. The theoretical picture is quantitatively supported by large-scale computer simulations of realistic frictional systems.

Author contributions: E.A.B. and E.B. designed research; A.P., E.A.B., and E.B. performed research; F.B. and T.R. helped with the numerical simulations; and A.P. and E.B. wrote the paper.

The authors declare no competing interest.

This article is a PNAS Direct Submission. J.F. is a guest editor invited by the Editorial Board.

[1]To whom correspondence may be addressed. Email: eran.bouchbinder@weizmann.ac.il or e.brener@fz-juelich.de.

This article contains supporting information online at https://www.pnas.org/lookup/suppl/doi:10.1073/pnas.2309374120/-/DCSupplemental.

Published August 17, 2023.

attracted toward and closely adhere to the $c_p^{(0)}[L^{(0)}]$ line. Consequently, one is able to understand the dynamics of unsteady slip pulses.

Furthermore, the unsteady dynamics along the $c_p^{(0)}[L^{(0)}]$ line are controlled by a single slow unstable mode. In particular, growing pulses feature $\dot{L}(t)/c_p(t) \ll 1$ and are nothing but sustained pulses that propagate many times their characteristic size without appreciably changing their properties. The $c_p^{(0)}[L^{(0)}]$ line is a dynamic attractor for unsteady slip pulses independently of their initial distance from the line, i.e., the theory applies to general initial conditions that lead to unsteady slip pulses. Our theoretical picture of unsteady frictional slip pulses is quantitatively supported by large-scale, dynamic boundary-integral method simulations for various initial conditions.

The Dynamic Stability of Steady-State Pulse Solutions

The frictional strength τ of contact interfaces depends on the time rate of change of the tangential displacement discontinuity across the interface, i.e., on the slip velocity $v(x,t)$ (here, x is the coordinate along the interface), and on the structural state of the interface. As macroscopic contact interfaces are never smooth on all scales (27, 29, 31, 33), a central structural state field is the real contact area, composed of an ensemble of contact asperities, which is typically orders of magnitude smaller than the nominal contact area (27, 33). Moreover, this scale separation between the real and nominal contact area implies that contact asperities experience intense loads and typically age with time. The aging time $\phi(x,t)$ is commonly used to quantify the nonequilibrium structural state of the interface (29, 31).

Consequently, the frictional strength is a functional $\tau[v(x,t),\phi(x,t)]$, whose form is extracted from experimental measurements and theoretical considerations (29, 31, 34); see Fig. 1. Finally, contact aging in the absence of sliding ($v=0$) and sliding-induced ($v>0$) rejuvenation (antiaging) are described as $\partial_t\phi(x,t) = 1 - v(x,t)\,\phi(x,t)/D$, where the transition between the two rheological behaviors is controlled by a characteristic slip displacement D (29, 31, 35–37). The frictional strength $\tau[v(x,t),\phi(x,t)]$ balances the shear stress emerging from the deformation of the bodies forming the contact interface, at any point x and time t. The deformable bodies extend in the y direction (the interface is located at $y=0$) and are assumed to be translationally invariant along the third direction z, making the problem considered here two-dimensional. When the bodies forming the contact interface are linear elastic and of infinite extent (or when the dynamics of interest are such that waves reflected from finite boundaries do not have time to affect the interface), the interfacial shear stress can be expressed in terms of the elastodynamic Green's function.

Considering then a frictional system driven antisymmetrically by a shear stress τ_d applied far from the interface, interfacial stress balance takes the form (38)

$$\tau[v(x,t),\phi(x,t)] = \tau_d - \frac{\mu}{2c_s}v(x,t) + s(x,t). \qquad [1]$$

Here, μ and c_s are the shear modulus and wave-speed of the bodies, respectively, and $s(x,t)$ is a spatiotemporal convolutional integral that accounts for the long-range interaction of different parts of the interface, mediated by bulk deformation. In general,

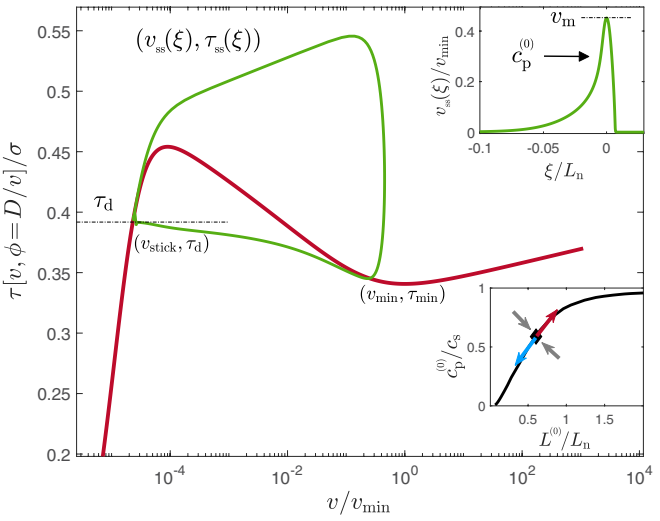

Fig. 1. (*Main*) The steady frictional resistance $\tau[v,\phi=D/v]$ (solid brown line, in units of the normal stress σ) vs. slip velocity v (in units of the v_{min}, the velocity at the local minimum). A steady-state slip pulse corresponds to a closed (homoclinic) orbit $(v_{ss}(\xi),\tau_{ss}(\xi))$ (solid green line) parameterized by the comoving space-time coordinate $\xi = x - c_p^{(0)}t$, where $c_p^{(0)}$ is the steady pulse propagation velocity. The closed orbit starts and ends at (v_{stick},τ_d), where τ_d is the driving shear stress and v_{stick} is extremely small. The existence of a minimum (v_{min},τ_{min}) of the friction curve, whose values are used to normalize various quantities, does not have a qualitative effect on the results. Yet, it might affect quantitative aspects of unsteady slip pulse propagation. (*Upper*) $v_{ss}(\xi)$, which features a maximal value v_m and a characteristic size $L^{(0)}$ (not marked, see *SI Appendix*), is plotted (ξ is expressed in units of L_n, a natural normalization length, see *SI Appendix*). (*Lower*) The size-velocity relation $c_p^{(0)}[L^{(0)}]$ (in units of the shear wave-speed c_s) for a family of steady-state pulse solutions parameterized by τ_d is plotted (solid line). A solution for a given τ_d is marked by the diamond, and its expected stability properties are represented by the arrows (see text for *Discussion*).

$s(x,t)$ does not admit an explicit real-space representation, and its specific form is different for antiplane shear symmetry (i.e., slip displacement in the z direction) and in-plane shear symmetry (i.e., slip displacement in the x direction) (39). Together with the $\partial_t\phi(x,t)$ equation stated above and an explicit expression for $\tau[v(x,t),\phi(x,t)]$ (see *SI Appendix* and Fig. 1), the coupled bulk-interface frictional dynamics are described by the specified set of nonlinear integro-differential equations.

Self-healing slip pulses correspond to solutions to the set of nonlinear integro-differential equations, which propagate at an instantaneous velocity $c_p(t)$ and feature a finite length $L(t)$. The compact support $L(t)$, over which slip velocities are large, separates two spatially homogeneous, nearly quiescent, identical interfacial states. The latter are characterized by a vanishingly small slip velocity $v_{stick} \to 0$ ("stick" denotes the fact that the state is nearly quiescent). It is obtained by solving $\tau_d = \tau[v_{stick}, D/v_{stick}]$ for a given driving shear stress τ_d, where $\phi = D/v$ corresponds to $\partial_t\phi = 0$. In the language of dynamical systems, self-healing slip pulses correspond to closed (homoclinic) orbits in the $v-\phi$ plane, which both start and end at $(v_{stick}, D/v_{stick})$. Alternatively, they correspond to closed (homoclinic) orbits in the $v-\tau$ plane, which both start and end at (v_{stick},τ_d), see Fig. 1.

Steady-state slip pulses correspond to solutions that also satisfy $c_p(t) = c_p^{(0)}$, i.e., which propagate steadily at a time-independent velocity $c_p^{(0)}$. Under such conditions, all fields depend on the comoving space-time coordinate $\xi \equiv x - c_p^{(0)}t$ and one has

$\partial_t = -c_p^{(0)}\partial_\xi$ (applied to the $\partial_t\phi(x,t)$ equation). Eq. **1** then takes the form (40)

$$\tau[v_{ss}(\xi), \phi_{ss}(\xi)] = \tau_d - \frac{\mu\,\mathcal{F}(c_p^{(0)}/c_s)}{c_p^{(0)}}\int_{-\infty}^{\infty}\frac{v_{ss}(z)}{z-\xi}dz, \qquad [2]$$

where the integral (which should be understood in the Cauchy principal value sense) is the steady-state limit of the two last terms on the right-hand-side of Eq. **1** and $\mathcal{F}(c_p^{(0)}/c_s)$ is a known function (different for antiplane and in-plane shear symmetries) (40).

A complete family of steady-state slip pulse solutions, i.e., $v_{ss}(\xi)$, $\phi_{ss}(\xi)$ and $c_p^{(0)}$ parameterized by τ_d, has been very recently obtained (25); see an example in the upper inset in Fig. 1. The properties of the solutions and their theoretical understanding have been discussed in ref. 25. Most relevant for our purposes here is that the family of steady-state slip pulse solutions features a size-velocity $L^{(0)}(\tau_d)-c_p^{(0)}(\tau_d)$ relation that is parameterized by τ_d, where $L^{(0)}$ is the characteristic size of each pulse (see *SI Appendix*). This relation is monotonically increasing and is plotted in the lower inset in Fig. 1 for antiplane shear symmetry and a representative set of frictional constitutive parameters (see *SI Appendix*).

In principle, the physical relevance of the obtained steady-state slip pulse solutions should be judged based on their dynamic stability. The above-formulated problem, which corresponds to bodies of infinite height H (i.e. $H\to\infty$), has been previously solved in the limit of small H (where long-range elastodynamic interactions become local) (21). It has been shown that steady-state slip pulses in this limit are intrinsically unstable, i.e., that $L^{(0)}(\tau_d)+\delta L$ perturbations (with $\delta L>0$) lead to growing pulses, while $L^{(0)}(\tau_d)-\delta L$ perturbations lead to decaying pulses. If the two problems are smoothly connected by continuously increasing H, we expect slip pulses in the $H\to\infty$ limit to be intrinsically unstable as well—in agreement with the existing literature (5, 22)—, i.e., to correspond to a saddle configuration for each τ_d. This expectation is tested next in the present context.

To test this expectation, we use the steady-state pulse solutions—$v_{ss}(\xi)$, $\phi_{ss}(\xi)$ and $c_p^{(0)}$ for a given τ_d—as initial conditions for the entire history $-\infty<t<0$ in Eq. **1** and for the $\partial_t\phi(x,t)$ equation, slightly perturb them in both directions ($\pm\delta L$) at $t=0$ and follow the subsequent dynamics using large-scale, dynamic boundary-integral method simulations (38, 41), using the open-source library cRacklet (42); see details in *SI Appendix*. The perturbation at $t=0$ takes the form $\phi(x,t=0)=(1+\epsilon)\phi(x,t=0^-)$. That is, we perturb the state field $\phi(x,t)$, where $\epsilon<0$ corresponds to $+\delta L$ perturbations and $\epsilon>0$ to $-\delta L$ ones. The results are presented in Fig. 2, where $L(t>0)$, $c_p(t>0)$ and the maximal slip velocity $v_m(t>0)$ (Fig. 1, *Upper*) are plotted for $\epsilon=-0.15$ and $\epsilon=-0.05$. It is observed that $\epsilon=-0.15$ gives rise to a growing pulse, while for $\epsilon=-0.05$ a decaying pulse emerges, where the transition from decay to growth takes place at ϵ_c in between. While theoretically we expect the transition to occur exactly at $\epsilon_c=0$, the numerical transition point is shifted by a few percent due to finite size effects and computational constraints (which limit the history duration; see *SI Appendix*).

The results in Fig. 2 show that steady-state pulses are intrinsically unstable and correspond to a saddle configuration, separating growing from decaying pulses. The characteristic timescale of variation of all 3 quantities ($L(t)$, $c_p(t)$, and $v_m(t)$), to be denoted by $\mathcal{T}$, appears to be similar. Focusing, for example, on the time evolution of $L(t)$ near $L^{(0)}(\tau_d)$, we expect it to follow the linearized dynamics

$$\dot{L}(t)=\frac{L(t)-L^{(0)}(\tau_d)}{\mathcal{T}(\tau_d)} \quad \text{for} \quad \frac{L(t)-L^{(0)}(\tau_d)}{L^{(0)}(\tau_d)}\ll 1. \qquad [3]$$

Moreover, a dimensional estimate suggests that $\mathcal{T}(\tau_d)\sim L^{(0)}(\tau_d)/c_p^{(0)}(\tau_d)$. These predictions are verified in Fig. 2*A*. Taken together, our results indicate that slip pulses are unsteady objects and that their dynamics near steady state is characterized by a single unstable mode, featuring an instability rate $\sim 1/\mathcal{T}(\tau_d)$.

Theory of Unsteady Frictional Slip Pulses

The unstable nature of steady-state slip pulses in large systems, established above, may suggest that steady-state slip pulse solutions are largely irrelevant for understanding the unsteady

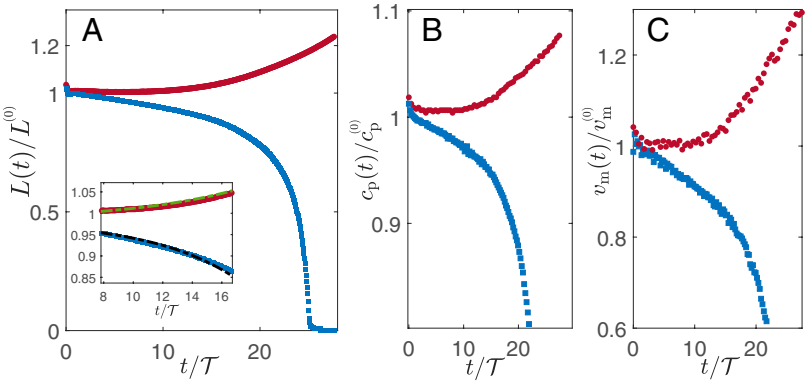

Fig. 2. Dynamic stability analysis of a steady-state pulse with $\tau_d=1.03\tau_{min}\approx 0.351\sigma$ (featuring $c_p^{(0)}=0.82c_s$) using the $\phi(x,t)$ field ϵ-perturbation scheme described in the text, with $\epsilon=-0.15$ (brown data) and $\epsilon=-0.05$ (blue data). (*A*) $L(t)/L^{(0)}$ vs. $t/\mathcal{T}$. (*B*) $c_p(t)/c_p^{(0)}$ vs. $t/\mathcal{T}$. (*C*) $v_m(t)/v_m^{(0)}$ vs. $t/\mathcal{T}$, with $\mathcal{T}=L^{(0)}/c_p^{(0)}$. For all 3 quantities, $\epsilon=-0.15$ (brown data) leads to growth and $\epsilon=-0.05$ (blue data) to decay, demonstrating the unstable nature of the steady-state pulse. The timescale of instability is similar in all quantities and is set by $\mathcal{T}$. In the inset of panel (*A*), we test the predicted unstable linearized dynamics in Eq. **3**. Since ϵ is not exactly centered around $\epsilon_c=0$, we consider the solution of Eq. **3** in the form $L_\pm(t)=L^{(0)}\pm\Delta L\exp[a_\pm(t-t_1)/\mathcal{T}]$ for $t>t_1$, with $t_1\simeq 8\mathcal{T}$, where $\pm$ correspond to the upper/lower branches, respectively. The results with $\Delta L/L^{(0)}\simeq 0.01$ (quantifying the deviation from steady state at t_1) are superimposed, for the upper branch with $a_+=0.13$ (green dashed-dotted line) and for the lower one with $a_-=0.17$ (black dashed-dotted line), supporting the prediction in Eq. **3**.

dynamics of slip pulses in realistic frictional systems. That is, the results show that slip pulses (under a fixed τ_d) that are initially close to $(L^{(0)}(\tau_d), c_p^{(0)}(\tau_d))$ are dynamically driven away from this point. Moreover, the obtained results appear to indicate that pulses that are unrelated to $(L^{(0)}(\tau_d), c_p^{(0)}(\tau_d))$, to begin with, will reveal no special relation to the $c_p^{(0)}[L^{(0)}]$ line, corresponding to unstable steady-state slip pulse solutions. If true, then, a theory of unsteady frictional slip pulses should be developed independently of steady-state slip pulse solutions (which is a formidable task). We show that this is in fact not the case. That is, while all of the above statements regarding the unstable steady-state point $(L^{(0)}(\tau_d), c_p^{(0)}(\tau_d))$ for a given τ_d are valid, the entire $c_p^{(0)}[L^{(0)}]$ line—parameterized by τ_d—is of fundamental importance for unsteady frictional slip pulses.

To understand this, let us consider pulse dynamics in the $L(t)-c_p(t)$ plane, where the steady-state $c_p^{(0)}[L^{(0)}]$ line is defined (Fig. 1, *Lower*). That is, while slip pulses are characterized by the fields $v(x,t)$ and $\phi(x,t)$, i.e., by infinitely many degrees of freedom, we are looking for a reduced-dimensionality description based on a small number of coarse-grained discrete variables, in particular, two such variables. The specific choice of $L(t)$ and $c_p(t)$ is physically motivated, as the pulse size and propagation velocity are of fundamental importance, yet it is by no means unique; in fact, we show that $L(t)$ and $v_m(t)$ could have been used as well (see *SI Appendix*). The two-dimensional dynamical system for $\dot{L}(t)$ and $\dot{c}_p(t)$ (under a given τ_d) is unknown and is in general nonlinear arbitrarily far from the point $(L^{(0)}(\tau_d), c_p^{(0)}(\tau_d))$.

Yet, the short-time dynamics near $(L^{(0)}(\tau_d), c_p^{(0)}(\tau_d))$ follow linearized equations as in Eq. **3** along its unstable direction. As the dynamical system is two-dimensional and there is one unstable mode (formally corresponding to a positive eigenvalue), the other mode is stable (corresponding to a negative eigenvalue). It is natural to expect the direction of the unstable mode in the $L(t)-c_p(t)$ plane to be along the local tangent to the $c_p^{(0)}[L^{(0)}]$ line at $(L^{(0)}(\tau_d), c_p^{(0)}(\tau_d))$ and the stable direction to be perpendicular to it, as is illustrated by the outgoing and ingoing arrows in Fig. 1, *Lower*. Plotting the results of Fig. 2 *A* and *B* in the $L(t)-c_p(t)$ plane (see *SI Appendix*) indeed shows that the unstable short-time dynamics near $(L^{(0)}(\tau_d), c_p^{(0)}(\tau_d))$ evolve along the local tangent to the $c_p^{(0)}[L^{(0)}]$ line at this point.

Since the above results apply to any point along the $c_p^{(0)}[L^{(0)}]$ line, a rather remarkable picture emerges. Invoking the continuity of dynamical trajectories in $L(t)-c_p(t)$ plane and assuming $c_p^{(0)}[L^{(0)}]$ to be the only steady-state line, we expect all dynamical trajectories that are away from the $c_p^{(0)}[L^{(0)}]$ line to be attracted to it, and once they hit it, say at time t_0, to evolve along the $c_p^{(0)}[L^{(0)}]$ line, whether corresponding to decaying or growing pulses. The latter implies that if one treats $L(t)$ as the "independent variable," we expect $c_p(t)$ to be determined according to

$$c_p(t) \simeq c_p^{(0)}[L(t)] \qquad \text{for} \qquad t > t_0, \qquad [4]$$

where the right-hand side of Eq. **4** is the steady-state relation $c_p^{(0)}[L^{(0)}]$ and its argument is the dynamic $L(t)$. Moreover, if $L(t_0) > L^{(0)}(\tau_d)$, then the pulse will grow ($\dot{L}(t>t_0)>0$), and if $L(t_0) < L^{(0)}(\tau_d)$, it will decay ($\dot{L}(t>t_0)<0$).

The emerging physical picture of unsteady slip pulses, to be quantitatively tested below, reveals that while each point $(L^{(0)}(\tau_d), c_p^{(0)}(\tau_d))$ along the steady-state $c_p^{(0)}[L^{(0)}]$ line is unstable in itself, i.e., the dynamics are repelled from it (as indicated by the arrows in Fig. 1, *Lower*), the entire steady-state $c_p^{(0)}[L^{(0)}]$ line is a dynamic attractor for unsteady slip pulses, whether decaying or growing.

Sustained slip pulses. Growing pulses are of particular importance as they are accompanied by large slip and radiated energy and hence would play major roles in the failure of frictional interfaces. Indeed, many experimental and numerical works demonstrate the existence of such unsteady slip pulses (3–24). It is observed that while these pulses are indeed out of steady state (as our theory predicts), they are nevertheless "sustained" in the sense that they propagate many times their characteristic size without appreciably changing their properties. Our theory of unsteady pulses may offer a natural explanation for sustained slip pulses. Clearly, we focus on pulses that correspond to $L(t_0) > L^{(0)}(\tau_d)$, leading to growth, i.e., $\dot{L}(t) > 0$ for $t > t_0$. If these are indeed sustained pulses, then the unstable mode (discussed above) that controls their growth should be a slow mode.

To quantify the possible slowness of the growing unstable mode, note that the time it takes a growing pulse to propagate a distance comparable to its own size is $\Delta t \simeq L(t)/c_p(t)$. The latter is valid if the change in size over this time $\Delta L(t) \simeq \Delta t\, \dot{L}(t)$ is much smaller than $L(t)$, which is a dimensionless measure of the slowness of the unstable mode. The expectation that $\Delta L(t) \ll L(t)$ amounts to

$$\dot{L}(t)/c_p(t) \ll 1 \qquad \text{for} \qquad \dot{L}(t) > 0 \qquad [5]$$

for $t > t_0$, which will be also quantitatively tested below.

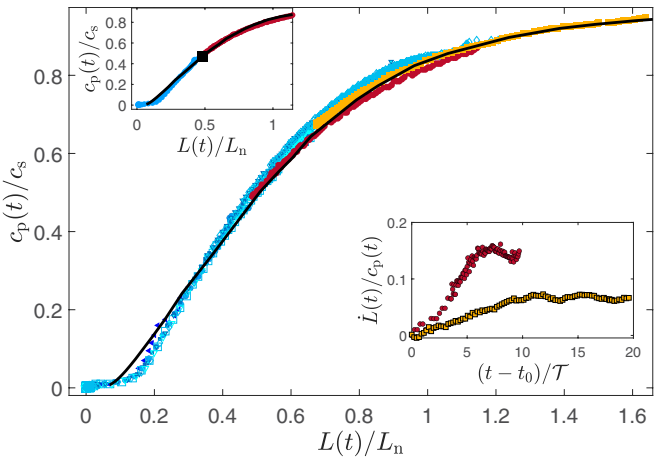

Fig. 3. (*Main*) $L(t)-c_p(t)$ trajectories corresponding to unsteady slip pulses generated from perturbed steady-state pulse solutions (various τ_d and ϵ perturbation values). It is observed that under all conditions, unsteady pulses (whether growing, marked in hot colors, or decaying, marked in cold colors) closely follow the steady-state $c_p^{(0)}[L^{(0)}]$ line (solid black line), if they are initially near it, as predicted in Eq. **4**. Shown are nine datasets, with τ_d/τ_{min} in the range $1.025-1.07$ and ϵ in the range -0.41 to 0 (see *SI Appendix*). The results for $\tau_d = 1.05\tau_{min}$ with $\epsilon = 0$ (decaying pulse, blue squares) and $\epsilon = -0.3$ (growing pulse, brown squares) are shown in the *Upper*. The steady-state $(L^{(0)}(\tau_d), c_p^{(0)}(\tau_d))$ point (black square) indeed separates growing from decaying pulses, as predicted. (*Lower*) $\dot{L}(t)/c_p(t)$ vs. $t-t_0$, verifying the prediction in Eq. **5** for growing pulses (see the scale of the y-axis).

Boundary-Integral Method Simulational Support

Our next goal is to quantitatively test the theoretical predictions discussed above in large-scale, dynamic boundary-integral method simulations (42 and *SI Appendix*). This is achieved in two steps. First, we aim at testing the predictions that: i) pulses that are initially close to the steady-state $c_p^{(0)}[L^{(0)}]$ line remain close to it at later times and ii) that the position of the initial point relative to $(L^{(0)}(\tau_d), c_p^{(0)}(\tau_d))$ determines whether a pulse grows or decays along the line.

Since steady-state pulse solutions reside on the $c_p^{(0)}[L^{(0)}]$ line (by definition), using perturbed steady-state pulse solutions as initial conditions is most suitable in the present context. We employ the same $\phi(x,t)$ field ϵ-perturbation scheme used above for the dynamic stability analysis (cf. Fig. 2 and the discussion related to it). In the Fig. 3, *Upper*, we present the results for two initial conditions for $\tau_d = 1.05\tau_{min}$ (a different value compared to Fig. 2), one (brown points) that features an up perturbation relative to the point $(L^{(0)}(\tau_d), c_p^{(0)}(\tau_d))$ (large black square) and another (blue points) that features a down perturbation relative to it. It is observed that the former becomes a growing pulse (increasing $L(t)$ and $c_p(t)$) and the latter becomes a decaying pulse (decreasing $L(t)$ and $c_p(t)$), as predicted. Moreover, and crucially, in both cases, the trajectory $L(t)-c_p(t)$ closely follows the steady-state $c_p^{(0)}[L^{(0)}]$ line (solid black line) at any time, as predicted theoretically in Eq. **4**.

Next, in the *Main* panel of Fig. 3, we superimpose $L(t)-c_p(t)$ trajectories for pulses obtained from steady-state solutions at various τ_d values and various ϵ perturbations [see figure caption, and note that the selected τ_d values are such that expanding crack-like rupture is not excited (21)]. Growing pulses appear in hot colors and decaying ones in cold colors. It is observed that independently of the value of τ_d and independently of whether the resulting pulse is growing or decaying, all unsteady pulse trajectories reside on the steady-state $c_p^{(0)}[L^{(0)}]$ line (solid black line) at any time, as predicted theoretically in Eq. **4**. Finally, in the *Lower*, we test the slow unstable growth prediction for growing pulses ($\dot{L}(t) > 0$, hot colors). It is observed that $\dot{L}(t)/c_p(t) \ll 1$ during the entire pulse propagation, as expected according to Eq. **5**. These results demonstrate that growing pulses along the $c_p^{(0)}[L^{(0)}]$ line are indeed sustained pulses.

In the second test of the theory, an even more stringent test, we aim at generating slip pulses that are initially arbitrarily far away from the steady-state $c_p^{(0)}[L^{(0)}]$ line. This will allow us to test the prediction that pulse trajectories in the $L(t)-c_p(t)$ plane are attracted to the $c_p^{(0)}[L^{(0)}]$ line, and once they hit it (say at time t_0), they remain close to the line at later times. Moreover, the resulting pulses are predicted to be growing or decaying depending on the position of the hitting point $(L(t_0), c_p(t_0))$ relative to $(L^{(0)}(\tau_d), c_p^{(0)}(\tau_d))$. The latter two predictions have already been verified in Fig. 3 for slip pulses that are initially close to the $c_p^{(0)}[L^{(0)}]$ line.

Slip pulses that are initially arbitrarily far from the $c_p^{(0)}[L^{(0)}]$ line are generated by introducing perturbations to a nearly quiescent frictional state (a state that slides at v_{stick}, i.e., at an extremely slow rate). The perturbations are initially stationary (i.e. nonpropagating) and may correspond to remote triggering processes and/or some interfacial heterogeneity. By varying the size of the perturbation, as explained in detail in *SI Appendix*, slip pulses of various properties can be generated.

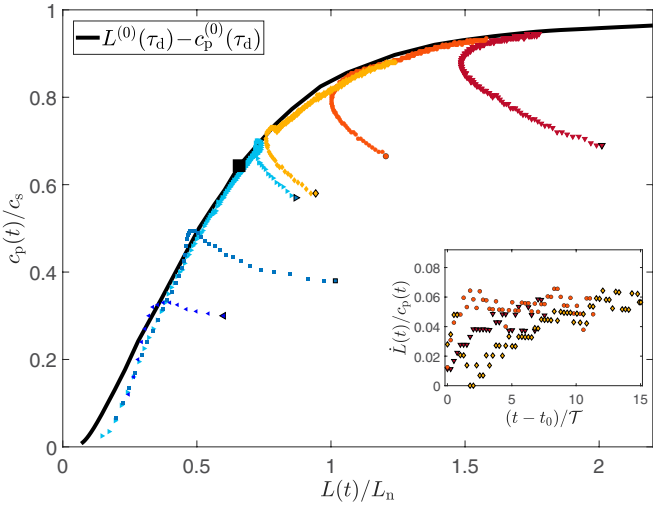

Fig. 4. The same as Fig. 3, but for 6 slip pulses that are initially far from the $c_p^{(0)}[L^{(0)}]$ line (solid black line), under a fixed $\tau_d = 1.04\tau_{min}$. Slip pulses are excited as detailed in the text and in *SI Appendix*, and their first time point is marked by a larger symbol in each case. It is observed that all pulse trajectories are attracted to the $c_p^{(0)}[L^{(0)}]$ line, and once hitting the line (at a time denoted as t_0), they remain close to it at any $t > t_0$ time. Moreover, the steady-state $(L^{(0)}(\tau_d), c_p^{(0)}(\tau_d))$ point (black square) separates growing (hot colors) from decaying (cold colors) pulses, as predicted. The prediction in Eq. **5** for growing pulses is verified in the inset (see the scale of the y-axis).

In Fig. 4, we present results for 6 different pulse trajectories in the $L(t)-c_p(t)$ plane for $\tau_d = 1.04\tau_{min}$. The first time at which well-defined slip pulse size L and propagation velocity c_p exist in each case is marked by a larger symbol. It is observed that while all pulse trajectories are initially far from the $c_p^{(0)}[L^{(0)}]$ line, they are dynamically attracted to it. Interestingly, the time it takes each pulse from formation to hitting the line is of order $\mathcal{T}(\tau_d)$ (see *SI Appendix*), indicating that the latter is a basic timescale in the pulse problem in a way that goes beyond the linearized dynamics of Eq. **3**. Once each trajectory hits the line (at time t_0), it remains close to it at any time. Moreover, the position of the hitting point relative to $(L^{(0)}(\tau_d), c_p^{(0)}(\tau_d))$ (large black square) approximately determines whether the dynamics along the line correspond to decaying pulses (cold colors) or to growing pulses (hot colors). For the latter, we find that $\dot{L}(t)/c_p(t) \ll 1$ for $t > t_0$ (see inset of Fig. 4), as expected according to Eq. **5**, demonstrating again that the growing pulses are indeed sustained pulses.

Summary and Discussion

A comprehensive theoretical picture of the dynamics of unsteady frictional slip pulses has been developed. We showed that steady-state slip pulses are intrinsically unstable objects, yet the steady-state line $L(\tau_d)-c_p(\tau_d)$ (parameterized by the driving stress τ_d) is of fundamental importance for unsteady pulse dynamics. In particular, while each point along the $c_p^{(0)}[L^{(0)}]$ line is unstable, the line itself is a dynamic attractor for pulses under a given τ_d.

Once a general pulse $L(t)-c_p(t)$ trajectory hits the $c_p^{(0)}[L^{(0)}]$ line, it remains close to it at any time. The position of the hitting point relative to $(L^{(0)}(\tau_d), c_p^{(0)}(\tau_d))$ determines whether

the dynamics along the line correspond to decaying or growing pulses. Finally, pulse dynamics along the $c_p^{(0)}[L^{(0)}]$ line are controlled by a single slow unstable mode, which for growing pulses is manifested by $\dot{L}(t)/c_p(t) \ll 1$. The latter corresponds to sustained pulses, which are of prime importance for the failure dynamics of frictional systems (21). The comprehensive theoretical picture has been quantitatively supported by large-scale, dynamic boundary-integral method simulations. We stress that we did not discuss here the conditions for exciting slip pulses (rather than expanding crack-like rupture), an issue that has been previously discussed in refs. 10, 17 and 21, but rather focused on their unsteady dynamics once they are excited.

The emerging theory suggests that the knowledge of the family of steady-state pulse solutions, in particular the steady-state line $L(\tau_d) - c_p(\tau_d)$, allows us to understand and predict many of the properties of unsteady slip pulses, when they are excited. The deep relation between unsteady slip pulses and their steady-state counterparts is valid for other discrete, coarse-grained variables (such as $L(t)$ and $v_m(t)$) and in fact also for the entire $v(x,t)$ and $\phi(x,t)$ fields themselves, as shown in *SI Appendix*. The theory also predicts the linearized dynamics near each unstable point, cf. Eq. **3**, with a characteristic timescale $\mathcal{T}(\tau_d) \sim L^{(0)}(\tau_d)/c_p^{(0)}(\tau_d)$. In fact, the timescale $\mathcal{T}(\tau_d)$ also characterizes the approach to the $c_p^{(0)}[L^{(0)}]$ line. Hence, $\mathcal{T}(\tau_d)$—which is also obtained from steady-state pulse solutions—appears to play the role of a basic timescale in the problem.

In addition, while the theory does not separately predict the general nonlinear dynamics of $\dot{L}(t)$ and $\dot{c}_p(t)$ along the line, their ratio is given as $\dot{L}(t)/\dot{c}_p(t) = (dc_p^{(0)}[L(t)]/dL(t))^{-1}$. Finally, Eq. **4** may be viewed as an equation of motion for unsteady pulses, where their velocity $c_p(t)$ instantaneously follows $L(t)$. This interpretation bears similarities to the equation of motion of ordinary cracks in bulk materials, where the crack's tip is viewed as a massless defect whose velocity instantaneously follows the crack length (43).

The numerical support to the theory, as presented above, employed a generic rate-and-state dependent friction law and antiplane symmetry conditions. We have no obvious reasons to expect any major/qualitative differences in the theoretical picture once different rate- and state-dependent friction laws (or frictional constitutive parameters) and in-plane symmetry conditions are considered. Yet, future work should test the emerging picture in a wider range of physical situations. Interestingly, the results presented in ref. 22 for a thermal pressurization constitutive relation indicate that unsteady slip pulses (when they are excited, and not expanding crack-like rupture) are related to the corresponding family of steady-state pulse solutions, similarly to our findings. The thermal pressurization results also indicate the relevance of the emerging picture to strongly weakening frictional interfaces, as well as to interfaces in which self-healing pulses do not depend on aging in stationary contact.

In general, knowledge of the interfacial constitutive relation (friction law) may allow one to come up with concrete predictions for unsteady pulse dynamics, which can be experimentally tested (e.g., in laboratory experiments). Future work should also address extensions of the present theory to inhomogeneous driving stresses.

Finally, in a broader context, the theory of the dynamics of unsteady slip pulses in frictional systems contributes to our general understanding of the dynamics of nonlinear spatially extended dissipative systems. This particularly pertains to the reduced-dimensionality description in terms of two coarse-grained dynamical variables, such as $L(t)$ and $c_p(t)$, whose dynamics are controlled by a single slow unstable mode. Such a theoretical picture bears some similarities to the dynamics of equilibrium first-order phase transitions, such as solidification (44), involving the formation of critical nuclei and front propagation in which a stable phase invades an unstable one (e.g., crystal growth in the solidification problem). In such cases, the dynamics are also dominated by a single slow unstable mode, which corresponds to the size of the growing nucleus.

Materials and Methods

The entire theory development is presented in the main text. Details of the interfacial constitutive relation (friction law) can be found in *SI Appendix*, section S-1. Details of the dynamic boundary-integral method simulations using the open-source library cRacklet can be found in *SI Appendix*, section S-2. Details of the two types of initial conditions used in the computer simulations and their implementation can be found in *SI Appendix*, section S-3. Details of how the dynamic evolution of unstable steady-state pulses is obtained can be found in *SI Appendix*, section S-4.

Data, Materials, and Software Availability. All study data are included in the article and/or *SI Appendix*.

ACKNOWLEDGMENTS. This work has been supported by the Israel Science Foundation (grant no. 1085/20). E.B. acknowledges support from the Ben May Center for Chemical Theory and Computation and the Harold Perlman Family.

Author affiliations: [a]Chemical and Biological Physics Department, Weizmann Institute of Science, Rehovot 7610001, Israel; [b]The Njord Centre, Department of Physics, University of Oslo, Oslo 0316, Norway; [c]The Njord Centre, Department of Geosciences, University of Oslo, Oslo 0316, Norway; [d]Civil Engineering Institute, Materials Science and Engineering Institute, Ecole Polytechnique Fédérale de Lausanne, Lausanne CH-1015, Switzerland; [e]Peter Grünberg Institut, Forschungszentrum Jülich, Jülich D-52425, Germany; and [f]Institute for Energy and Climate Research, Forschungszentrum Jülich, Jülich D-52425, Germany

1. Y. Ben-Zion, Dynamic ruptures in recent models of earthquake faults. *J. Mech. Phys. Solids* **49**, 2209–2244 (2001).
2. C. H. Scholz, *The Mechanics of Earthquakes and Faulting* (Cambridge University Press, 2002).
3. L. B. Freund, The mechanics of dynamic shear crack propagation. *J. Geophys. Res.* **84**, 2199 (1979).
4. T. H. Heaton, Evidence for and implications of self-healing pulses of slip in earthquake rupture. *Phys. Earth Planet. Inter.* **64**, 1–20 (1990).
5. G. Perrin, J. R. Rice, G. Zheng, Self-healing slip pulse on a frictional surface. *J. Mech. Phys. Solids* **43**, 1461–1495 (1995).
6. G. C. Beroza, T. Mikumo, Short slip duration in dynamic rupture in the presence of heterogeneous fault properties. *J. Geophys. Res. Solid Earth* **101**, 22449–22460 (1996).
7. N. M. Beeler, T. E. Tullis, Self-healing slip pulses in dynamic rupture models due to velocity-dependent strength. *Bull. Seismol. Soc. Am.* **86**, 1130–1148 (1996).
8. A. C. and R. Madariaga, Complexity of seismicity due to highly rate-dependent friction. *J. Geophys. Res. Solid Earth* **101**, 25321–25336 (1996).
9. D. J. Andrews, Y. Ben-Zion, Wrinkle-like slip pulse on a fault between different materials. *J. Geophys. Res. Solid Earth* **102**, 553–571 (1997).
10. G. Zheng, J. R. Rice, Conditions under which velocity-weakening friction allows a self-healing versus a cracklike mode of rupture. *Bull. Seismol. Soc. Am.* **88**, 1466–1483 (1998).
11. S. B. Nielsen, J. M. Carlson, Kim B. Olsen, Influence of friction and fault geometry on earthquake rupture. *J. Geophys. Res. Solid Earth* **105**, 6069–6088 (2000).
12. S. Nielsen, R. Madariaga, On the self-healing fracture mode. *Bull. Seismol. Soc. Am.* **93**, 2375–2388 (2003).
13. E. A. Brener, S. V. Malinin, V. I. Marchenko, Fracture and friction: Stick-slip motion. *Eur. Phys. J. E* **17**, 101–113 (2005).
14. Z. Shi, Y. Ben-Zion, A. Needleman, Properties of dynamic rupture and energy partition in a solid with a frictional interface. *J. Mech. Phys. Solids* **56**, 5–24 (2008).
15. A. M. Rubin, J.-P. Ampuero, Self-similar slip pulses during rate-and-state earthquake nucleation. *J. Geophys. Res.* **114**, B11305 (2009).
16. D. I. Garagash, Seismic and aseismic slip pulses driven by thermal pressurization of pore fluid. *J. Geophys. Res. Solid Earth* **117**, B04314 (2012).
17. A.-A. Gabriel, J.-P. Ampuero, L. A. Dalguer, P. M. Mai, The transition of dynamic rupture styles in elastic media under velocity-weakening friction. *J. Geophys. Res. Solid Earth* **117**, B09311 (2012).

18. J. Galetzka *et al*., Slip pulse and resonance of the Kathmandu basin during the 2015 Gorkha earthquake, Nepal. *Science* **349**, 1091–1095 (2015).
19. T. Putelat, J. H. P. Dawes, A. R. Champneys, A phase-plane analysis of localized frictional waves. *Proc. R. Soc. A* **473**, 20160606 (2017).
20. S. Michel, J.-P. Avouac, N. Lapusta, J. Jiang, Pulse-like partial ruptures and high-frequency radiation at creeping-locked transition during megathrust earthquakes. *Geophys. Res. Lett.* **44**, 8345–8351 (2017).
21. E. A. Brener, M. Aldam, F. Barras, J.-F. Molinari, E. Bouchbinder, Unstable slip pulses and earthquake nucleation as a nonequilibrium first-order phase transition. *Phys. Rev. Lett.* **121**, 234302 (2018).
22. N. Brantut, D. I. Garagash, H. Noda, Stability of pulse-like earthquake ruptures. *J. Geophys. Res. Solid Earth* **124**, 998–9020 (2019).
23. V. Lambert, N. Lapusta, S. Perry, Propagation of large earthquakes as self-healing pulses or mild cracks. *Nature* **591**, 252–258 (2021).
24. T. Roch, E. A. Brener, J.-F. Molinari, E. Bouchbinder, Velocity-driven frictional sliding: Coarsening and steady-state pulses. *J. Mech. Phys. Solids* **158**, 104607 (2022).
25. A. Pomyalov, Y. Lubomirsky, L. Braverman, E. A. Brener, E. Bouchbinder, Self-healing solitonic slip pulses in frictional systems. *Phys. Rev. E* **107**, L013001 (2023).
26. J. H. Dieterich, Time-dependent friction and the mechanics of stick-slip. *Pure Appl. Geophys.* **116**, 790–806 (1978).
27. J. H. Dieterich, B. D. Kilgore, Direct observation of frictional contacts: New insights for state-dependent properties. *Pure Appl. Geophys.* **143**, 283–302 (1994).
28. N. M. Beeler, T. E. Tullis, J. D. Weeks, The roles of time and displacement in the evolution effect in rock friction. *Geophys. Res. Lett.* **21**, 1987–1990 (1994).
29. C. Marone, Laboratoty-derived friction laws and their application to seismic faulting. *Annu. Rev. Earth Planet. Sci.* **26**, 643–696 (1998).
30. P. Berthoud, T. Baumberger, C. G'Sell, J.-M. Hiver, Physical analysis of the state- and rate-dependent friction law: Static friction. *Phys. Rev. B* **59**, 14313–14327 (1999).
31. T. Baumberger, C. Caroli, Solid friction from stick-slip down to pinning and aging. *Adv. Phys.* **55**, 279–348 (2006).
32. O. Ben-David, S. M. Rubinstein, J. Fineberg, Slip-stick and the evolution of frictional strength. *Nature* **463**, 76 (2010).
33. F. P. Bowden, D. Tabor, *The Friction and Lubrication of Solids* (Oxford University Press, 2001), vol. 1.
34. Y. Bar-Sinai, R. Spatschek, E. A. Brener, E. Bouchbinder, On the velocity-strengthening behavior of dry friction. *J. Geophys. Res. Solid Earth* **119**, 1738–1748 (2014).
35. J. H. Dieterich, Modeling of rock friction: 2. Simulation of preseismic slip. *J. Geophys. Res.* **84**, 2169 (1979).
36. A. L. Ruina, Slip instability and state variable friction laws. *J. Geophys. Res.* **88**, 10359–10370 (1983).
37. M. Nakatani, Conceptual and physical clarification of rate and state friction: Frictional sliding as a thermally activated rheology. *J. Geophys. Res. Solid Earth* **106**, 13347–13380 (2001).
38. S. Das, A numerical method for determination of source time functions for general three-dimensional rupture propagation. *Geophys. J. Int.* **62**, 591–604 (1980).
39. M. S. Breitenfeld, P. H. Geubelle, Numerical analysis of dynamic debonding under 2D in-plane and 3D loading. *Int. J. Fract.* **93**, 13–38 (1998).
40. J. Weertman, Unstable slippage across a fault that separates elastic media of different elastic constants. *J. Geophys. Res. Solid Earth* **85**, 1455–1461 (1980).
41. P. Geubelle, J. R. Rice, A spectral method for three-dimensional elastodynamic fracture problems. *J. Mech. Phys. Solids* **43**, 1791–1824 (1995).
42. T. Roch, F. Barras, P. H. Geubelle, J.-F. Molinari, cRacklet: A spectral boundary integral method library for interfacial rupture simulation. *J. Open Source Softw.* **7**, 3724 (2022).
43. L. B. Freund, *Dynamic Fracture Mechanics* (Cambridge University Press, Cambridge, 1998).
44. E. M. Lifschitz, L. P. Pitajewski, *"Physical Kinetics" in Course of Theoretical Physics* (Pergamon Press, 1983), vol. 10, chap. XII.